

New Class of Drug Modalities: Directed Evolution of a De Novo Designed Helix–Loop–Helix Peptide to Bind VEGF for Tumor Growth Inhibition

Masataka Michigami, Tharanga M. R. Ramanayake Mudiyansele, Miho Suzuki, Hirotsugu Ishizako, Kunpei Notsu, Kikuya Sugiura, and Ikuo Fujii*



Cite This: *ACS Chem. Biol.* 2022, 17, 647–653



Read Online

ACCESS |



Metrics & More

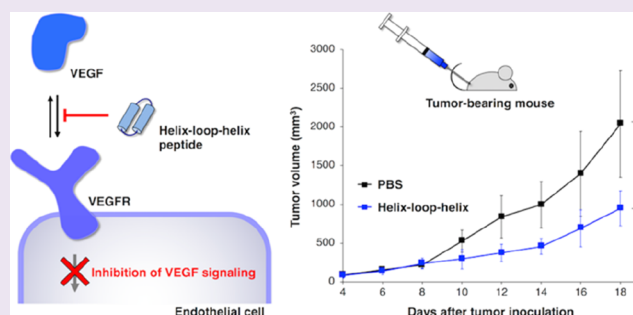


Article Recommendations



Supporting Information

ABSTRACT: As a small affinity molecule to serve as an alternative to antibodies, we have developed a conformationally constrained peptide with a de novo designed helix–loop–helix (HLH) scaffold. To evaluate its potential for biomedical applications, we performed directed evolution of HLH peptides to obtain an inhibitor for vascular endothelial growth factor-A (VEGF). A phage-displayed library of HLH peptides was constructed and screened against VEGF, giving the peptide VS42 that inhibits the VEGF/VEGF receptor-2 interaction ($IC_{50} = 210$ nM), which was further improved by in vitro affinity maturation using a yeast-displayed library. An identified HLH peptide, VS42-LR3, exhibited improved inhibitory activity ($IC_{50} = 37$ nM), high thermal stability, and excellent resistance against chemical denaturation. In biological activity tests, the HLH peptide was found to block VEGF-induced proliferation of human umbilical vein endothelial cells and suppress tumor growth in a murine xenograft model of human colorectal cancer.



INTRODUCTION

At present, monoclonal antibodies are the most successful agents in molecular-targeted therapy.^{1,2} However, antibodies have limitations such as high immunogenicity and high cost and complexity of manufacture. Because these drawbacks are due to their large molecular size (~150 kDa) and complicated molecular composition, it is of great interest to develop downsized alternative affinity molecules with non-immunoglobulin folds.³ Using naturally occurring protein scaffolds, a variety of small proteins have been engineered such as DARPin (~21 kDa),⁴ anticalin (~20 kDa),⁵ monobody (~10 kDa),⁶ and truncated Z-domain.⁷ To address further downsizing, we have developed a conformationally constrained peptide with a de novo designed helix–loop–helix (HLH) structure termed “molecular targeting HLH peptide” (~4 kDa).⁸ The HLH peptide is too small to induce an unwanted immunogenic reaction and is resistant to enzymatic degradation. HLH peptides, which consist of natural L-amino acids, have the advantage of synthetic simplicity and can be produced by conventional chemical synthesis at low cost.

In the HLH peptide scaffold YT1-S (Figure 1A), eight leucine residues inside the two helices facilitate a hydrophobic interaction, which is the driving force to fold the peptide into the HLH structure, and an intramolecular disulfide bond between the N- and C-termini plays an accessory role in structure stabilization. On the other hand, the solvent-exposed

residues have no contributions to the peptide folding. Therefore, random mutations are introduced into the solvent-exposed positions in YT1-S to give a library of peptides with the HLH structure. Previously, we constructed phage-displayed libraries of HLH peptides, which were screened against a variety of disease-related proteins to develop molecular targeting HLH peptides with antibody-like affinity and specificity.^{9,10}

In this work, we demonstrate the generation of an HLH peptide inhibitor for human vascular endothelial growth factor-A (VEGF) from the HLH peptide libraries. VEGF is a well-established molecular target for cancer therapy.¹¹ Some tumor cells overexpress VEGF, which interacts with the VEGF receptor to stimulate angiogenesis. Because tumor angiogenesis is essential for tumor growth and metastasis, a VEGF-neutralizing antibody, bevacizumab, is widely used for cancer therapy. Although VEGF peptide inhibitors were previously

Received: November 29, 2021

Accepted: February 8, 2022

Published: February 18, 2022



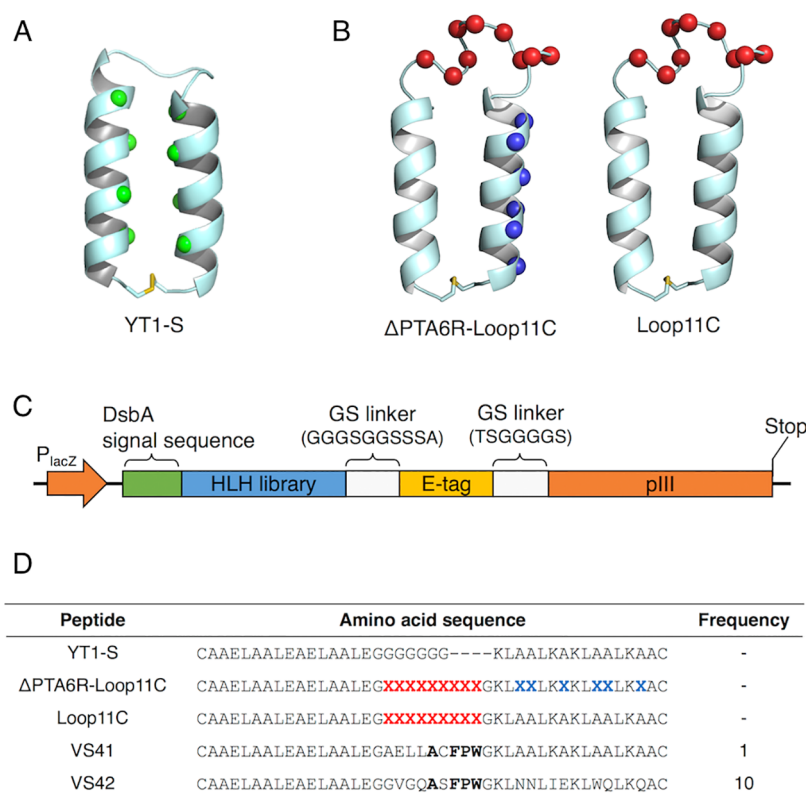


Figure 1. Design of the phage-displayed HLH peptide libraries. (A) Structural models of the HLH peptide scaffold. Leu residues in a hydrophobic core are represented green spheres. (B) Structural models of the HLH peptide libraries. The Δ PTA-6R-Loop11C library has a 43 amino acid length composed of the N-terminal helix (AELAALAEALAELE, 14 aa), loop (GXXXXXXXXXG, 11 aa), C-terminal helix (KLXXLKXXLXXLXX, 14 aa), and AC linkers at both termini. The randomized positions are presented as red and blue spheres. (C) Gene arrangement of the phagemid vector. (D) Amino acid sequence of HLH peptide libraries and identified clones. The number of identified clones is indicated as frequency.

developed by phage display,^{12,13} their anticancer effects in vivo have not been described.

Here, we report on the screening process of the HLH peptide libraries and the biochemical characterization of selected VEGF-targeting peptides (binding affinity and structural stability) and describe their VEGF-blocking activities in vitro and in vivo using human umbilical vein endothelial cells (HUVECs) and a LS174T human colorectal cancer xenograft model.

RESULTS AND DISCUSSION

Screening of Phage-Displayed HLH Peptide Libraries.

Two types of phage-displayed HLH peptide library, Δ PTA-6R-Loop11C and Loop11C, were constructed based on the HLH peptide scaffold YT1-S and screened against VEGF to isolate HLH peptide inhibitors (Figure 1B). In library Δ PTA-6R-Loop11C, the peptide loop region was randomized using NNK degenerate codons, and the C-terminal α -helical region was randomized by using NDK degenerate codons to avoid encoding Pro, Thr, and Ala because proline residues break an α -helical structure. In library Loop11C, only the loop region was randomized using NNK degenerate codons. These peptide libraries were displayed on the minor coat protein pIII of the M13 phage by modification of the pComb3 system.^{14–16} To detect peptide expression on phage surfaces by enzyme-linked immunosorbent assay (ELISA), an E-tag (GAPVPYPD-PLEPR) was inserted into a GS linker between the peptide C-terminus and the pIII protein (Figure 1C).

These phage libraries were mixed with biotinylated VEGF. Phage clones binding to VEGF were captured by streptavidin-linked magnetic beads followed by competitive elution with recombinant human VEGF receptor-2 (VEGFR-2). After four rounds of screening, we confirmed the enrichment of VEGF-binding phages by phage ELISA (Figure S1), and the binding phage clones were randomly picked up for DNA sequencing. Consequently, two peptide candidates, VS41 and VS42, which possessed the consensus sequence (AXFPW, X = C and S) in the loop region, were identified (Figure 1D), and peptide V42 with a higher frequency was examined in more detail.

Peptide VS42 was synthesized by Fmoc solid-phase peptide synthesis (SPPS) (Figure S2). The peptide cyclization reaction proceeded to give VS42 in a high yield (~70%), and there was no detection for the formation of the oligomers with intermolecular disulfide bonds. This suggested that the linear peptide folded into the HLH structure, in which the cysteine residues at both termini were close enough to promote the intramolecular disulfide bond formation. The chemically synthesized VS42 was examined for its binding affinity to VEGF and inhibition activity against the VEGF/VEGFR-2 interaction by surface plasmon resonance (SPR). As a result, VS42 showed a dissociation constant (K_D) of 401 ± 22 nM and an IC_{50} value of 210 ± 2 nM for the VEGF/VEGFR-2 interaction (Figures S3A and S4).

The phage-displayed peptide libraries were screened against VEGF to give HLH peptides binding to VEGF. Consequently, first, the binding affinity (K_D values) was determined. However, the binding affinity gave no guarantee of inhibitory

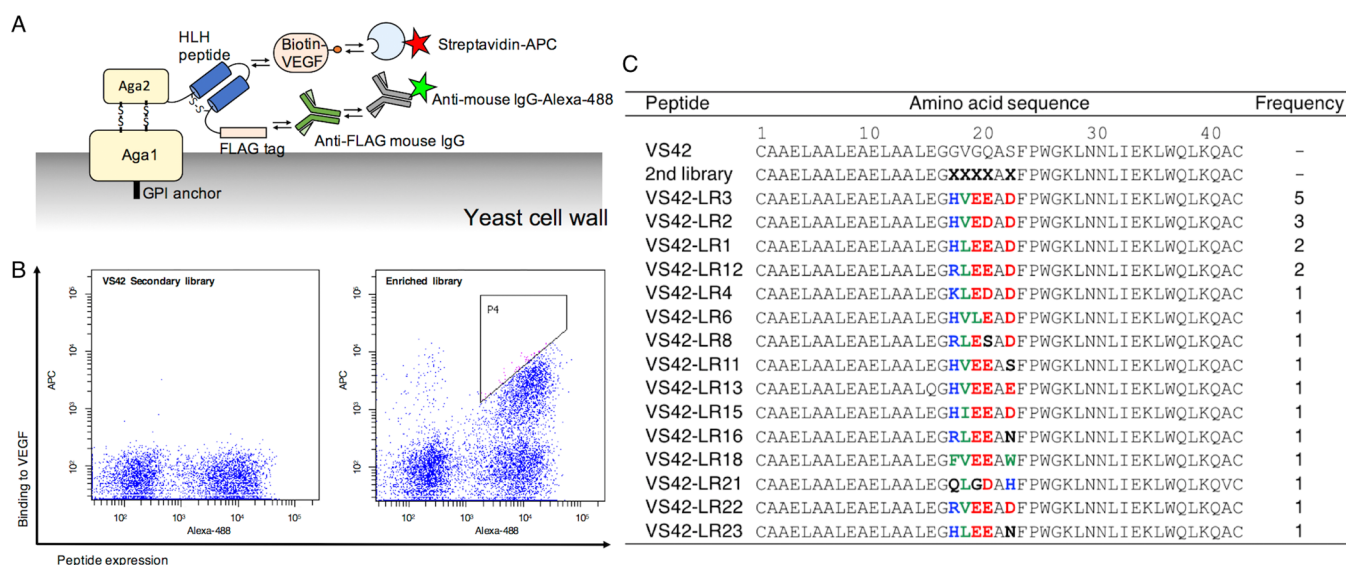


Figure 2. In vitro affinity maturation of the VS42 peptide. (A) Fluorescent labeling of the yeast library for FACS screening. The peptide expression and target binding were monitored using Alexa-488 and APC, respectively. (B) Flow cytometric analysis of the VS42 secondary library and the enriched yeast library. (C) List of HLH peptides isolated from the VS42 secondary library. The basic amino acid residues, hydrophobic residues, and acidic residues are indicated as blue, green, and red, respectively. The number of identified clones is shown as the frequency.

Table 1. Summary of Biophysical Properties of the HLH Peptides

peptide	sequence	K_D (nM)	IC_{50} (nM)	$t_{1/2}$ (min)
Loop11C	CAAEAALEAEALAALEGGXXXXXXXXXGKLAALKAKLAALKAAC			
Δ PTA-6R-Loop11C	CAAEAALEAEALAALEGGXXXXXXXXXGKLLXKXKLLXKXAC			
YT1-S	CAAEAALEAEALAALEGGGGGGGKLAALKAKLAALKAYC	N.D. ^a	N.D.	N.T. ^b
VS42	CAAEAALEAEALAALEGGVQASFPWGKLNLIKWLKQAC	392 ± 22	210 ± 2	N.T.
VS42-LR3	CAAEAALEAEALAALEGHVVEADFPWGKLNLIKWLKQAC	74.9 ± 0.9	36.6 ± 7.1	1670 ± 10
VS42-LR3-dN	GHVEEADFPWGKLNLIKWLKQ	N.D.	N.T.	2.01 ± 0.02

^aN.D.: not determined. The peptide was tested but no measurable value was observed. ^bN.T.: not tested.

activity for VEGF/VEGFR-2 interaction: the inhibitory activity should require a competitive binding to the receptor-binding site of VEGF. Therefore, in the next step, inhibitory activity (IC_{50} values) for VEGF/VEGFR-2 interaction was examined. In the previous work, we isolated a VEGF-targeting HLH peptide, M49, by bio-panning with library Δ PTA-6R-Loop11C in which the binding phage particles were eluted under acidic conditions (glycine-HCl buffer, pH = 2.0).¹⁰ The peptide M49 showed tight binding to VEGF ($K_D = 0.87$ nM), but no inhibitory activity for the VEGF/VEGFR interaction. Therefore, we conjugated M49 with a toxin to generate a peptide–drug conjugate, which made a ternary complex with VEGF and VEGFR to go into cells by receptor-mediated endocytosis. In the current work, VEGF-binding peptides were screened by bio-panning in which the binding phage particles were eluted by excess of its receptor (VEGFR). The competitive elution led to the success of selecting a peptide inhibitor for the VEGF/VEGFR interaction.

In Vitro Affinity Maturation of Peptide VS42. To improve the binding affinity of VS42, we performed in vitro affinity maturation in yeast surface-displayed libraries. This display system offers an advantage in that yeast cells can be sorted using fluorescence-activated cell sorting (FACS), allowing quantitative discrimination among peptide mutants with different binding affinities.¹⁷ The isolated peptides, VS41 and VS42, possessed the consensus sequence in the loop region (AXFPW, X = C/S), which was likely to be significant for VEGF binding. Therefore, we introduced random

mutations in five amino acid (aa) residues located near the consensus sequence in VS42 (CAAEAALEAEALAALEGGXXXXXFPWGKLNLIKWLKQAC, X = any natural amino acid, and the consensus sequence is underlined). The size of the constructed yeast library was estimated as 2.4×10^7 from the number of yeast transformants. We performed two rounds of magnetic-activated cell sorting (MACS) to amplify the VEGF binders. The library was labeled with biotinylated VEGF and captured by streptavidin microbeads, followed by magnetic separation. In the second round, anti-biotin microbeads were used to exclude the yeast cells binding to streptavidin. After MACS, the enrichment of the affinity binders was confirmed by flow cytometry: yeast cells binding biotinylated VEGF (50 nM) were labeled with streptavidin-APC (Figure 2A). As shown in Figure 2B, the APC signal of the VS42 library before MACS was comparable to the background, and in contrast, the enriched yeast library after MACS exhibited high fluorescence from APC. This indicated that high-affinity clones were successfully enriched by screening with MACS. Finally, we sorted the yeast cells in the P4 gate by FACS (Figure 2B). Some of the sorted cells were randomly picked up for DNA sequencing, and the deduced peptide sequences were similar (Figure 2C). At position 18, the Gly residue of VS42 was substituted with positively charged amino acids (His, Arg, or Lys). At position 19, hydrophobic residues such as Val, Ile, and Leu were conserved, and this site of the wild-type is also a hydrophobic residue, Val. At the other three positions, 20, 21, and 23, negatively charged amino acid residues frequently

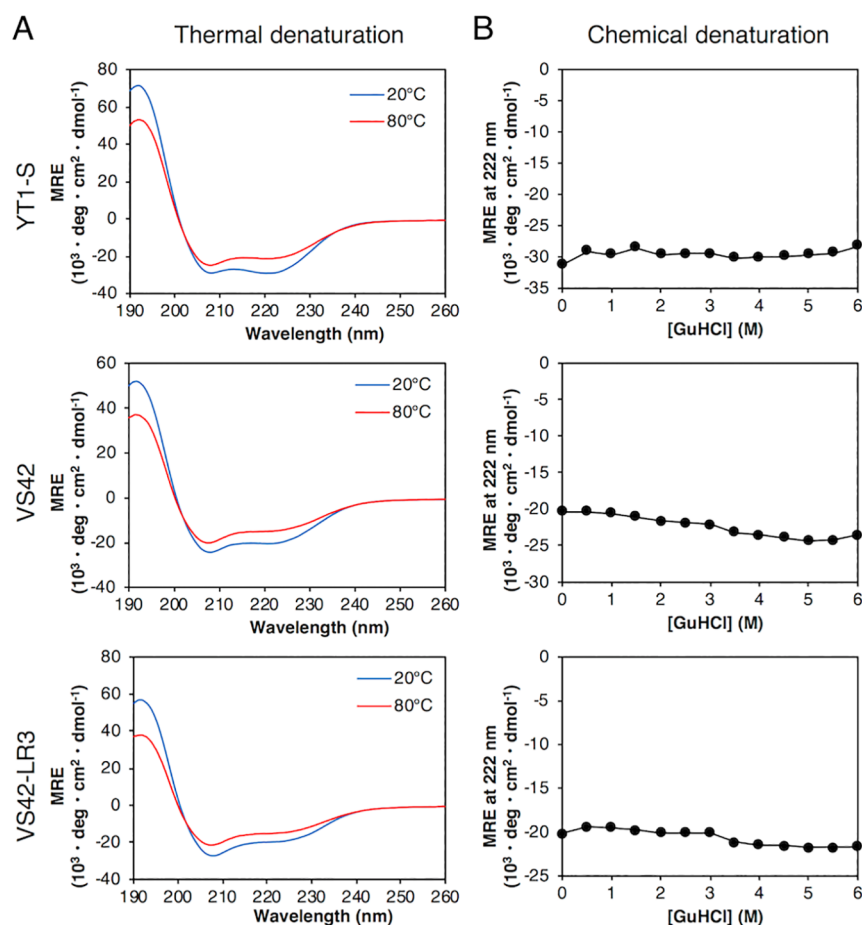


Figure 3. Structural stability of the HLH peptides. (A) CD spectra of the HLH peptides at 20 and 80 °C in 10 mM phosphate buffer at pH 7.4. CD spectra are presented as mean residue ellipticity. (B) Changes in MRE at 222 nm with the increase in concentrations of GuHCl are shown.

appeared. VS41, an isolated peptide from the first library, possesses a Cys residue in the loop region at position 23 that has the potential to form a dimer by a disulfide bond. However, majority of sorted peptides from the second library presented Asp, and Cys did not appear at position 23. Thus, the dimeric formation by Cys23 would not be significant for the VEGF binding. A peptide with high frequency, VS42-LR3, was synthesized by Fmoc SPPS, and the binding affinity was determined by SPR. As shown in Table 1, peptide VS42-LR3 exhibited improved binding affinity ($K_D = 74.9 \pm 0.9$ nM) and inhibition activity ($IC_{50} = 36.6 \pm 7.1$ nM) for the VEGF/VEGFR-2 interaction.

Peptide Structural Stability. Historically, native peptides have been disfavored as drug leads owing to their short plasma half-life.¹⁸ Peptides are susceptible to proteolysis by proteases or peptidases, which is a major elimination pathway from the body. Therefore, the HLH peptides were designed to maintain a well-folded stable conformation to provide proteolytic resistance. We evaluated the structural stability and proteolytic stability of the HLH peptides. As shown in CD spectral measurements (Figure 3A), at 20 °C, peptides YTI1-S, VS42, and VS42-LR3 showed typical CD spectra of an α -helical structure. Even at 80 °C, these HLH peptides maintained an α -helical structure, although the ellipticities at 222 nm slightly increased. Similarly, in GuHCl denaturation experiments, no changes in the ellipticities of the HLH peptides were observed (Figure 3B). Thus, despite the randomized mutations on the C-terminal helix and the loop region, the isolated HLH

peptides from the library had stable α -helical structures, as same as that of the library scaffold YTI1-S.

Previously, peptides with a two-helical bundle, Z34C and mini-Z have been designed as a truncated version of the Z-domain of protein A and used for a scaffold for phage-displayed libraries.^{7,13} The HLH peptide and Z34C have totally different amino acid sequences, but share structural similarities with the HLH fold. The most significant difference is the positions of a hydrophobic core contributing to the formation of stable tertiary structures. Z34C has hydrophobic residues, which are clustered on one edge of the helical interface. The clustered hydrophobic residues are enclosed by charged residues in the solvent-exposed region to enhance the hydrophobic interaction and solubilities.¹⁹ On the other hand, the HLH peptide has hydrophobic residues, which pack tightly inside the interface between the two helices. This difference is most likely to affect the thermal stability of the tertiary structures. The temperature dependence of the CD spectrum for Z34C showed a complete denaturation at 80 °C,¹⁹ while the HLH peptides maintained an α -helical structure at 80 °C, as shown in Figure 3A.

Next, we examined the stability of peptides against trypsin by HPLC analysis. Deletion of the N-terminal helical region of VS42-LR3 gave a random-coil peptide (Figure S5), which showed a half-life of 2.01 ± 0.02 min. In contrast, the HLH peptide VS42-LR3 exhibited an 830-fold increased trypsin resistance (Table 1 and Figure S6). A variety of strategies have been developed to stabilize peptides, such as introducing N-

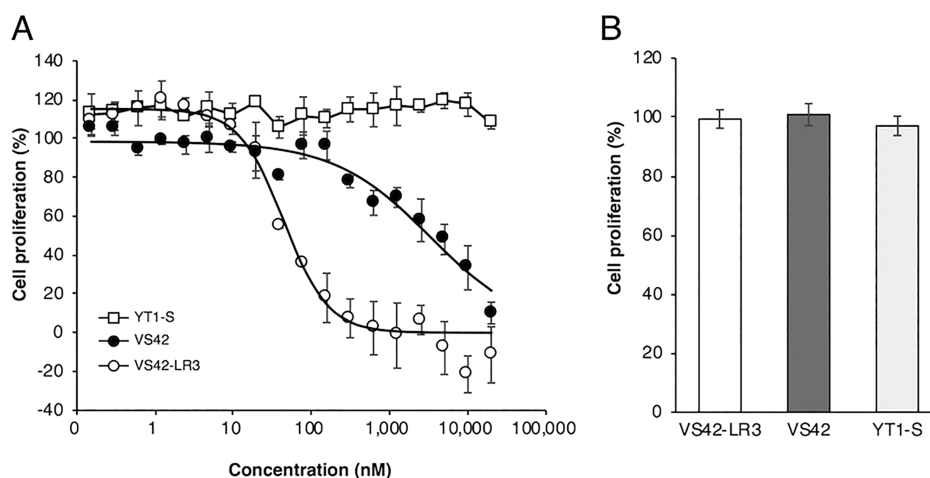


Figure 4. Cell growth inhibition by VEGF inhibitory HLH peptides. (A) Inhibition of VEGF-induced HUVEC proliferation. (B) Inhibition of bFGF-induced HUVEC proliferation. 20 micromolar HLH peptides were incubated with bFGF (25 ng/mL). After 24 h incubation, cell viability was measured using WST-1. The data represent the means of triplicate experiments and standard deviation.

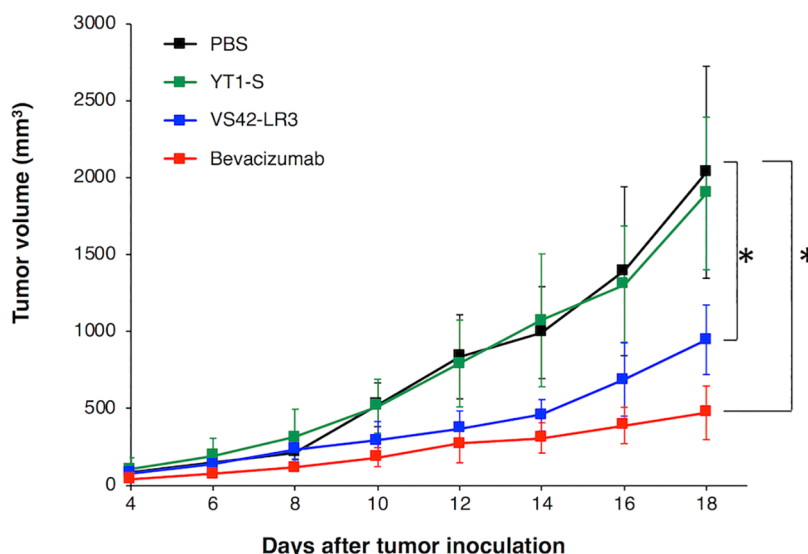


Figure 5. Tumor growth inhibition by the HLH peptides. LS174T cells were inoculated into BALB/c nude mice. The mice were treated with bevacizumab (5 mg/kg on days, 1, 4, 7, and 10) or the HLH peptides (10 mg/kg on days 1–10). Data represent mean \pm standard deviation ($n = 5$). * $p < 0.01$ vs control.

alkylation and replacing with D- and β -amino acids.²⁰ Although the HLH peptides are only composed of natural L-amino acids, the well-folded stable conformation provides strong proteolytic resistance to improve peptide druggability.

Cell-Based Assays. To investigate the inhibition activity of the HLH peptides against angiogenesis, we performed VEGF-induced proliferation assays using HUVECs. In the assay, HUVECs were stimulated by VEGF in the presence of HLH peptides, and after cell cultivation, the cell viability was determined using WST-1 reagent. As a result, peptides VS42 and VS42-LR3 exhibited antiproliferative activity in a dose-dependent manner, with IC_{50} values of 3300 nM and 44 nM, respectively, while the scaffold peptide YT1-S showed no effect on proliferation (Figure 4A). In contrast, when basic fibroblast growth factor (bFGF) was used to stimulate HUVECs, the HLH peptides exhibited no antiproliferative activity (Figure 4B), showing that they were specific for VEGF.

In Vivo Tumor Growth Inhibition. Finally, the ability of VS42-LR3 to inhibit tumor growth was examined with a

murine xenograft model: LS174T human colorectal cancer cells were subcutaneously transplanted into BALB/c nude mice. The day after the tumor inoculation, phosphate-buffered saline (PBS), YT1-S (10 mg/kg), or VS42-LR3 (10 mg/kg) was administered intraperitoneally (i.p.) every day for 10 days. An anti-VEGF antibody drug, bevacizumab (5.0 mg/kg), was used as a positive control and i.p. administered every 3 days four times as previously reported.²¹ Because small-sized peptides generally suffer rapid renal filtration,²² VS42-LR3 was administered at a higher dose and shorter dosing interval as compared to bevacizumab.

As shown in Figure 5, the HLH peptide VS42-LR3 and bevacizumab both inhibited tumor growth. The tumor volumes were significantly smaller than in PBS-treated mice ($p < 0.01$). Although the peptide administration was ended at day 10, VS42-LR3 inhibited tumor growth at the same level as bevacizumab until day 14, and still significantly inhibited it at day 18 compared with PBS and YT1-S as a control peptide.

CONCLUSIONS

Therapeutic antibodies are a successful class of molecular-targeted drugs. However, their applications are limited owing to their biophysical properties, large molecular size, and molecular complexity. As an alternative to antibodies, we have developed a downsized binding peptide with a de novo designed HLH structure.

Herein, we successfully isolated the VEGF-binding HLH peptide VS42-LR3 to inhibit a ligand–receptor interaction by directed evolution of our original HLH peptide libraries. In the construction of these libraries, the amino acid residues used for random mutations and their mutated positions were controlled to maintain the constrained HLH structure. Consequently, the isolated peptides possessed extremely stable α -helical structures that have potential as molecular-targeted drugs with high binding affinity, specificity, and proteolytic resistance. This preorganized, constrained conformation limits the unfavorable entropy loss during the interaction with VEGF, thus resulting in strong binding affinity. The constrained conformation also limits the adoption of a binding conformation to other proteins and to the active sites of any proteases, resulting in target specificity and proteolytic resistance.

Finally, we revealed that the HLH peptide VS42-LR3 possesses VEGF-neutralizing activity and shows anticancer effects in a xenograft model of LS174T human colorectal cancer. HLH peptides have great potential as an alternative to antibodies for molecular-targeted therapy. However, in general, such small-sized peptides suffer rapid renal filtration. Therefore, further investigations of the pharmacokinetics profile of the HLH peptide and improvements in blood retentivity by advanced technology drug delivery systems would lead to practical applications.

METHODS

Phage Display. The phage-displayed HLH peptide libraries were incubated with biotinylated VEGF₁₆₅ in 3% bovine serum albumin (BSA)-containing PBS. We captured VEGF-bound phages by Dynabeads M-280 Streptavidin (Invitrogen). After washing with PBST (PBS with 0.05% Tween 20), VEGF-bound phages were eluted with a recombinant human VEGFR-2/Fc chimera (R&D systems) for 15 min at room temperature. The recovered phages were amplified at 30 °C in XL1-Blue with VCSM13 helper phage for the subsequent round of bio-panning.

Yeast Surface Display. The yeast surface-displayed HLH peptide library was mixed with biotinylated VEGF₁₆₅ for 1 h. After washing with PBSM (PBS with 0.5% BSA), the cells were incubated with streptavidin-coupled microbeads for 1 h. After washing with PBSM, we resuspended the cells in 7 mL of PBSM and separated VEGF-bound yeast cells using an LS column. The collected cells were grown in SDCAA at 30 °C for 18 h and cultured in SG/RCAA at 20 °C for 20 h to express the HLH peptides on the yeast cell surface.

In FACS screening, the yeast library was incubated with mouse anti-FLAG antibody (Sigma) and biotinylated VEGF for 1 h. After washing with PBST, the cells were labeled with goat anti-mouse IgG antibody Alexa 488 (Thermo Fisher Scientific) and streptavidin-APC (Thermo Fisher Scientific) for 1 h. Cell sorting was performed on a BD FACS Aria II. The sorted yeast cells were spread on an SD (–Ura, –Trp) plate.

Cell-Based Assays. HUVECs (Lonza) were seeded in gelatin-coated 96-well microplates (5000 cells/100 μ L/well) in EBM-2 and stimulated by 25 ng/mL recombinant human VEGF₁₆₅ or bFGF (R&D Systems) in the presence of HLH peptides for 48 h. Then, 10 μ L of WST-1 (Roche) was added into each well to determine the cell proliferation. Data represent mean \pm standard deviation of three independent experiments.

In Vivo Tumor Growth Inhibition. LS174T cells were expanded in EMEM supplemented 10% FBS. On day 0, LS174T cells (1×10^6) were transplanted subcutaneously into BALB/c nude mice. The mice were injected i.p. with 5 mg/kg bevacizumab every 3 days for a total of four doses (days 1, 4, 7, and 10) or treated with daily injections of the HLH peptides at 10 mg/kg (i.p. administration: days 1–10). The tumor volume was calculated according to the formula: (longest diameter) \times (short diameter)² \times 0.5. Mice were killed when the tumor volume reached 2000 mm³.

All research staff involved in the animal experiments received training in animal care, and experiments were approved by the Animal Experiment Committee of Osaka Prefecture University.

ASSOCIATED CONTENT

Supporting Information

The Supporting Information is available free of charge at <https://pubs.acs.org/doi/10.1021/acscchembio.1c00940>.

Additional experimental methods; screening of the phage-displayed HLH peptide libraries against VEGF-A; RP-HPLC profiles and MALDI-TOF-MS spectra of the synthetic HLH peptides; binding affinity for the interaction between the HLH peptides and VEGF-A₁₆₅; SPR-based inhibition assay; CD spectra; and peptide stabilities against trypsin (PDF)

AUTHOR INFORMATION

Corresponding Author

Ikuo Fujii – Department of Biological Science, Graduate School of Science, Osaka Prefecture University, Sakai, Osaka 599-8531, Japan; orcid.org/0000-0003-2571-546X; Email: fujii@b.s.osakafu-u.ac.jp

Authors

Masataka Michigami – Department of Biological Science, Graduate School of Science, Osaka Prefecture University, Sakai, Osaka 599-8531, Japan

Tharanga M. R. Ramanayake Mudiyansele – Department of Veterinary Science, Graduate School of Life and Environmental Science, Osaka Prefecture University, Izumisano, Osaka 598-8531, Japan

Miho Suzuki – Department of Biological Science, Graduate School of Science, Osaka Prefecture University, Sakai, Osaka 599-8531, Japan

Hirotsugu Ishizako – Department of Biological Science, Graduate School of Science, Osaka Prefecture University, Sakai, Osaka 599-8531, Japan

Kunpei Notsu – Department of Biological Science, Graduate School of Science, Osaka Prefecture University, Sakai, Osaka 599-8531, Japan

Kikuya Sugiura – Department of Veterinary Science, Graduate School of Life and Environmental Science, Osaka Prefecture University, Izumisano, Osaka 598-8531, Japan

Complete contact information is available at:

<https://pubs.acs.org/doi/10.1021/acscchembio.1c00940>

Notes

The authors declare no competing financial interest.

ACKNOWLEDGMENTS

This research was supported by the Platform Project for Supporting Drug Discovery and Life Science Research [Basis for Supporting Innovative Drug Discovery and Life Science Research (BINDS)] from the Japan Agency for Medical

Research and Development (AMED) under Grant Number JP19am0101097.

REFERENCES

- (1) Kaplon, H.; Muralidharan, M.; Schneider, Z.; Reichert, J. M. Antibodies to Watch in 2020. *mAbs* **2020**, *12*, 1703531.
- (2) Urquhart, L. Top Companies and Drugs by Sales in 2019. *Nat. Rev. Drug Discovery* **2020**, *19*, 228.
- (3) Binz, H. K.; Amstutz, P.; Plückthun, A. Engineering Novel Binding Proteins from Nonimmunoglobulin Domains. *Nat. Biotechnol.* **2005**, *23*, 1257–1268.
- (4) Forrer, P.; Stumpp, M. T.; Binz, H. K.; Plückthun, A. A Novel Strategy to Design Binding Molecules Harnessing the Modular Nature of Repeat Proteins. *FEBS Lett.* **2003**, *539*, 2–6.
- (5) Beste, G.; Schmidt, F. S.; Stibora, T.; Skerra, A. Small Antibody-like Proteins with Prescribed Ligand Specificities Derived from the Lipocalin Fold. *Proc. Natl. Acad. Sci. U.S.A.* **1999**, *96*, 1898–1903.
- (6) Koide, A.; Bailey, C. W.; Huang, X.; Koide, S. The Fibronectin Type III Domain as a Scaffold for Novel Binding Proteins. *J. Mol. Biol.* **1998**, *284*, 1141–1151.
- (7) Braisted, A. C.; Wells, J. A. Minimizing a binding domain from protein A. *Proc. Natl. Acad. Sci. U.S.A.* **1996**, *93*, 5688–5692.
- (8) Suzuki, N.; Fujii, I. Optimization of the Loop Length for Folding of a Helix-Loop-Helix Peptide. *Tetrahedron Lett.* **1999**, *40*, 6013–6017.
- (9) Mudiyansele, T. M. R. R.; Michigami, M.; Ye, Z.; Uyeda, A.; Inoue, N.; Sugiura, K.; Fujii, I.; Fujiwara, D. An Immune-Stimulatory Helix-Loop-Helix Peptide: Selective Inhibition of CTLA-4-B7 Interaction. *ACS Chem. Biol.* **2020**, *15*, 360–368.
- (10) Michigami, M.; Takahashi, K.; Yamashita, H.; Ye, Z.; Nakase, I.; Fujii, I. A “Ligand-Targeting” Peptide-Drug Conjugate: Targeted Intracellular Drug Delivery by VEGF-Binding Helix-Loop-Helix Peptides via Receptor-Mediated Endocytosis. *PLoS One* **2021**, *16*, No. e0247045.
- (11) Ellis, L. M.; Hicklin, D. J. VEGF-Targeted Therapy: Mechanisms of Anti-Tumour Activity. *Nat. Rev. Cancer* **2008**, *8*, 579–591.
- (12) Fairbrother, W. J.; Christinger, H. W.; Cochran, A. G.; Fuh, G.; Keenan, C. J.; Quan, C.; Shriver, S. K.; Tom, J. Y. K.; Wells, J. A.; Cunningham, B. C. Novel peptides selected to bind vascular endothelial growth factor target the receptor-binding site. *Biochemistry* **1998**, *37*, 17754–17764.
- (13) Fedorova, A.; Zobel, K.; Gill, H. S.; Ogasawara, A.; Flores, J. E.; Tinianow, J. N.; Vanderbilt, A. N.; Wu, P.; Meng, Y. G.; Williams, S.-P.; Wiesmann, C.; Murray, J.; Marik, J.; Deshayes, K. The development of peptide-based tools for the analysis of angiogenesis. *Chem. Biol.* **2011**, *18*, 839–845.
- (14) Barbas, C. F.; Kang, A. S.; Lerner, R. A.; Benkovic, S. J. Assembly of Combinatorial Antibody Libraries on Phage Surfaces: The Gene III Site. *Proc. Natl. Acad. Sci. U.S.A.* **1991**, *88*, 7978–7982.
- (15) Takahashi, N.; Kakinuma, H.; Liu, L.; Nishi, Y.; Fujii, I. In Vitro Abzyme Evolution to Optimize Antibody Recognition for Catalysis. *Nat. Biotechnol.* **2001**, *19*, 563–567.
- (16) Fujii, I.; Fukuyama, S.; Iwabuchi, Y.; Tanimura, R. Evolving Catalytic Antibodies in a Phage-Displayed Combinatorial Library. *Nat. Biotechnol.* **1998**, *16*, 463–467.
- (17) Feldhaus, M. J.; Siegel, R. W.; Opresko, L. K.; Coleman, J. R.; Feldhaus, J. M. W.; Yeung, Y. A.; Cochran, J. R.; Heinzelman, P.; Colby, D.; Swers, J.; Graff, C.; Wiley, H. S.; Wittrup, K. D. Flow-Cytometric Isolation of Human Antibodies from a Nonimmune *Saccharomyces Cerevisiae* Surface Display Library. *Nat. Biotechnol.* **2003**, *21*, 163–170.
- (18) Otvos, L.; Wade, J. D. Current Challenges in Peptide-Based Drug Discovery. *Front. Chem.* **2014**, *2*, 62.
- (19) Starovasnik, M. A.; Braisted, A. C.; Wells, J. A. Structural mimicry of a native protein by a minimized binding domain. *Proc. Natl. Acad. Sci. U.S.A.* **1997**, *94*, 10080–10085.
- (20) Yao, J.-F.; Yang, H.; Zhao, Y.-Z.; Xue, M. Metabolism of Peptide Drugs and Strategies to Improve their Metabolic Stability. *Curr. Drug Metabol.* **2018**, *19*, 892–901.
- (21) Varey, A. H. R.; Rennel, E. S.; Qiu, Y.; Bevan, H. S.; Perrin, R. M.; Raffy, S.; Dixon, A. R.; Paraskeva, C.; Zaccaro, O.; Hassan, A. B.; Harper, S. J.; Bates, D. O. VEGF 165 b, an antiangiogenic VEGF-A isoform, binds and inhibits bevacizumab treatment in experimental colorectal carcinoma: balance of pro- and antiangiogenic VEGF-A isoforms has implications for therapy. *Br. J. Cancer* **2008**, *98*, 1366–1379.
- (22) Holeček, M. J. Glomerular filtration: an overview. *Nephrol. Nurs. J.* **2003**, *30*, 285.

Recommended by ACS

Efficacy Evaluation of SDF-1 α -Based Polypeptides in an Acute Myocardial Infarction Model Using Structure-Based Drug Design

Kang-Gon Lee, Yongdoo Park, *et al.*

SEPTEMBER 30, 2022

ACS BIOMATERIALS SCIENCE & ENGINEERING

READ 

Exploring the Surface of the Ectodomain of the PD-L1 Immune Checkpoint with Small-Molecule Fragments

Radoslaw Kitel, Bogdan Musielak, *et al.*

SEPTEMBER 08, 2022

ACS CHEMICAL BIOLOGY

READ 

Enzymatic Macrolactamization of mRNA Display Libraries for Inhibitor Selection

Matthew M. Bowler, Albert A. Bowers, *et al.*

DECEMBER 09, 2022

ACS CHEMICAL BIOLOGY

READ 

Phage Display Selected Cyclic Peptide Inhibitors of Kallikrein-Related Peptidases 5 and 7 and Their *In Vivo* Delivery to the Skin

Patrick Gonschorek, Christian Heinis, *et al.*

JUNE 02, 2022

JOURNAL OF MEDICINAL CHEMISTRY

READ 

Get More Suggestions >